Cancer Management and Research

Elevate Series

Open Access Full Text Article

ORIGINAL RESEARCH

Analysis of the Diagnostic Efficacy and Clinical Utility of Multiparametric MRI in Prostate Cancer Diagnosis

Xiongbo Lou

Department of Radiology, General Hospital of Traditional Chinese Medicine Hospital of Keqiao District, Shaoxing, Zhejiang, 312030, People's Republic of China

Correspondence: Xiongbo Lou, Email Louxiongbo@126.com

Objective: To evaluate the diagnostic efficacy and clinical relevance of multiparametric MRI (mpMRI) in detecting prostate cancer (PCA).

Methods: This retrospective study analyzed 64 patients with suspected PCA who underwent MRI and were pathologically diagnosed with either PCA (n=33) or benign prostatic lesions (BPL, n=31). Imaging characteristics were assessed using T2-weighted imaging (T2WI), diffusion-weighted imaging (DWI), and dynamic contrast-enhanced MRI (DCE-MRI). DWI signal intensities at b=50 and b=800s/mm² and apparent diffusion coefficient (ADC) values were compared. Perfusion parameters, including Ktrans, Ve, and Kep, were also analyzed. Spearman correlation assessed associations between imaging parameters and PCA occurrence. Receiver operating characteristic (ROC) curves evaluated the diagnostic performance of each sequence and their combination.

Results: PCA lesions showed hypointensity on T2WI, hyperintensity on DWI, and type II/III curves on DCE-MRI. Signal intensities at b=50 and b=800s/mm² and ADC values were significantly lower in PCA than in BPL ($P < 0.05$), whereas Ktrans, Ve, and Kep were significantly higher ($P < 0.05$). Spearman analysis showed negative correlations between PCA occurrence and b=50, b=800 signal intensities and ADC ($r = –0.547, –0.529, –0.601$), and positive correlations with Ktrans, Ve, and Kep ($r = 0.516, 0.538, 0.552$; all $P < 0.05$). ROC analysis revealed AUCs of 0.834 (T2WI), 0.819 (DWI), 0.696 (DCE-MRI), and 0.902 (combined T2WI+DWI), with the combined approach yielding the highest diagnostic accuracy.

Conclusion: mpMRI parameters including DWI signal intensity, ADC, and DCE-MRI perfusion values are significantly associated with PCA. Combined application of T2WI and DWI improves diagnostic accuracy and may offer greater clinical value than individual sequences.

Keywords: multiparametric MRI, prostate cancer, correlation, diagnostic efficacy, clinical utility

Introduction

Prostate cancer (PCA) is one of the most common malignant tumors among men worldwide. Although its incidence varies across regions, there has been a general upward trend, particularly among elderly men.[1] According to global cancer statistics, PCA ranks among the leading causes of morbidity and mortality in male malignancies, significantly impacting patients' quality of life[2] Due to the often atypical early symptoms of PCA, many patients are diagnosed at an advanced stage, which limits treatment options and effectiveness.[3,4] Therefore, improving the early detection rate of PCA is crucial for enhancing patient prognosis. However, current routine screening and diagnostic methods for PCA have several limitations. Digital rectal examination (DRE) is highly dependent on the operator's experience, while prostate-specific antigen (PSA) testing has low specificity and is prone to interference from benign prostatic hyperplasia (BPH) or prostatitis, leading to high false-positive and false-negative rates. Although transrectal ultrasound (TRUS)-guided prostate biopsy remains the gold standard for diagnosis, it is an invasive procedure with potential sampling bias and may result in missed diagnoses due to tumor heterogeneity.[5–7] Consequently, there is an urgent need for a more accurate, non-invasive, or minimally invasive imaging technique for PCA detection.

In recent years, magnetic resonance imaging (MRI) has become increasingly important in the diagnosis of prostate diseases, particularly multiparametric MRI, which provides anatomical, cellular, and hemodynamic information about prostate tissue. It has shown great potential in the detection, grading, and prognosis evaluation of PCA.[8,9]

Received: 28 May 2025
Accepted: 18 August 2025
Published: 27 August 2025

Multiparametric MRI includes T2-weighted imaging (T2WI), diffusion-weighted imaging (DWI), and dynamic contrast-enhanced MRI (DCE-MRI). Among them, T2WI offers clear visualization of the prostate's internal structure and provides critical anatomical information about lesions.[10] DWI assesses the diffusion motion of water molecules in tissues, indirectly reflecting cellular density.[11] DCE-MRI evaluates tumor microvascular characteristics based on contrast agent enhancement patterns, providing essential information for distinguishing PCA from benign lesions.[12] However, despite the growing use of mpMRI and the establishment of standardized reporting systems such as PI-RADS v2.1,[13] there remains ongoing debate over the relative diagnostic value and reproducibility of individual parameters such as ADC values, perfusion metrics (Ktrans, Kep), and their thresholds for distinguishing PCA from benign prostatic lesions (BPL).[14,15] Studies have reported variations in the sensitivity and specificity of different sequences depending on lesion location, tumor grade, and reader experience.[16] Moreover, quantitative DCE-MRI parameters show promise but remain underutilized due to technical variability and lack of standardization.[17] Therefore, the diagnostic efficiency of individual mpMRI parameters and their combined application in routine clinical settings requires further investigation.

To address this gap, this study retrospectively analyzed the multiparametric MRI data of 64 patients with suspected PCA in our hospital. The aim was to optimize the imaging evaluation framework for PCA, enhance the clinical utility of mpMRI, and provide a more reliable imaging-based strategy for the early and accurate diagnosis of PCA.

Data and Methods

Basic Data

A retrospective analysis was conducted on the clinical data of 64 patients with suspected PCA who were admitted to our hospital between April 2022 and October 2024. All patients were male and exhibited varying degrees of acute urinary retention, difficulty urinating, frequent urination, nocturia, or painless gross hematuria. Inclusion criteria: (1) Abnormal clinical manifestations, serum PSA levels, or imaging findings indicating potential prostate lesions, with a possibility of PCA, and undergoing MRI examination; (2) All patients underwent prostate biopsy or postoperative pathological examination and were ultimately diagnosed with either PCA or benign prostatic lesions (BPL); (3) All patients underwent T2WI, DWI (b = 50s/mm² and b = 800s/mm²), and DCE-MRI, with complete and analyzable imaging data available; (4) Patients had not received surgery, radiotherapy, chemotherapy, or hormone therapy prior to MRI examination, ensuring that imaging characteristics were not affected by treatment; (5) Patients and their families were informed about the study, provided consent, and signed relevant informed consent forms; (6) Patients had complete clinical records, imaging data, pathological reports, and laboratory test results available for statistical analysis. Exclusion criteria: (1) Patients whose imaging had significant artifacts, motion artifacts, or excessive signal attenuation, preventing accurate assessment of lesion characteristics; (2) Patients with other urinary system or systemic malignancies that could affect PCA imaging findings; (3) Patients with acute prostatitis or systemic infections meeting ≥2 SIRS criteria (temperature >38°C or <36°C, heart rate >90/min, respiratory rate >20/min, WBC $>12\times10^9$/L or $<4\times10^9$/L);[18] (4) Patients with a history of prior prostate surgery that could influence MRI imaging findings; (5) Patients unable to tolerate contrast agent injection (eg, severe renal failure, eGFR < 30 mL/min/1.73 m²) and thus unable to complete the DCE-MRI scan; (6) Patients with a history of contrast agent allergy or other contraindications to MRI contrast-enhanced examination; (7) Patients lacking complete pathological reports or MRI examination data, making a comprehensive analysis impossible.

Sample Size Justification: A pre-study power analysis (G*Power 3.1) indicated that 60 patients provided 85% power to detect AUC differences ≥0.15 between diagnostic methods (α=0.05, two-tailed), based on expected AUCs from prior mp-MRI studies.[19] Our final sample (n=64) exceeded this requirement.

Pathological diagnosis: All patients underwent a combined biopsy protocol, consisting of a 12-core systematic transrectal ultrasound (TRUS)-guided biopsy and an MRI-targeted biopsy of lesions with a PI-RADS score ≥3, performed using the UroNav fusion system. The procedures were conducted in accordance with the STARD guidelines.[20] Postoperative histopathological analysis confirmed prostate cancer (PCA) in 33 cases and benign prostatic lesions (BPL) in 31 cases.

This study was approved by the Medical Ethics Committee of the General Hospital of Traditional Chinese Medicine, Keqiao District, Shaoxing City (Approval Number: NKYX2427), and was conducted in strict accordance with the ethical guidelines outlined in the Declaration of Helsinki.

Methods

Examination Methods

All patients in this study were not required to undergo bladder filling before the examination. Imaging was performed using a SIEMENS Altea 1.5T MRI system equipped with an 8-channel phased-array abdominal coil. The scanning process included T2WI, DWI, and DCE-MRI to comprehensively evaluate the imaging characteristics of the prostate tissue.

Conventional T1WI and T2WI Scanning

A wide-range pelvic scan was initially performed to clarify the anatomical structures of the prostate and surrounding tissues and to assess whether distant metastases were present. A fast spin-echo (FSE) sequence was used to acquire axial, sagittal, and coronal images for multi-angle evaluation. T2WI acquisition parameters: Repetition time (TR): 3420 ms, Echo time (TE): 98 ms, Slice thickness: 5 mm, Slice gap: 1 mm, Field of view (FOV): 24×24 cm. T1WI was performed in axial and coronal planes to further aid in the characterization of lesions and the anatomical details of the prostate.

DWI

DWI was performed using a dual-excitation echo-planar imaging (EPI) sequence in axial and sagittal planes. DWI scan parameters: TR: 3200 ms, TE: 84 ms, Matrix size: 256 × 256, Slice thickness: 3 mm, Slice gap: 0.3 mm, FOV: 400 mm × 400 mm. To enhance the differentiation of prostate tumors, two different b-values were used, b = 50s/mm² and b = 800s/mm², to assess signal variations in lesion areas and to calculate apparent diffusion coefficient (ADC) values.

DCE-MRI

DCE-MRI was performed using a LAVA sequence for volumetric scanning and to analyze signal variation patterns over time. Axial, sagittal, and coronal scans were conducted. DCE-MRI scan parameters: TR: 145 ms, TE: 4.76 ms, Echo train length: 1, FOV: 300 mm × 300 mm, Matrix: 64 × 256, Slice thickness: 5 mm, Slice gap: 2.5 mm, Single scan time: 12s. The contrast agent gadobutrol was intravenously injected via the median cubital vein at a dosage of 0.1 mL/kg, with an injection flow rate of 2.5 mL/s, followed by the initiation of dynamic contrast-enhanced scanning. DCE-MRI was performed in seven repeated scans, with a 5-second interval between scans, to fully record the dynamic signal changes in the prostate tissue after the contrast agent entered the systemic circulation and to generate enhancement curves.

Image Data Analysis and Processing

All imaging data in this study were analyzed using the SIEMENS ADW4.4 workstation, primarily evaluating the morphological characteristics, imaging signal features, and functional parameters of prostate lesions. The image analysis process included observation of basic imaging characteristics, quantitative parameter calculation, and multimodal image fusion processing. (1) Imaging Feature Evaluation: Researchers first observed the morphology, size, number, edge characteristics, signal intensity, and surrounding tissue conditions of the lesions on the original MRI images (T2WI, DWI, and DCE-MRI). They also assessed whether there was invasion of adjacent structures or lymph node metastasis. The analysis of morphological characteristics aimed to preliminarily determine tumor invasiveness and provide a basis for subsequent quantitative analysis. (2) Region of Interest (ROI) Delineation and Quantitative Parameter Calculation: To obtain objective numerical indicators of the lesion area, Functool 4.3 software was used for image post-processing, and Tissue 4D software was applied to extract parameters related to dynamic contrast-enhanced MRI. The specific operations were as follows: ① DWI Image Processing: Researchers manually delineated the ROI in the lesion area on DWI images, while selecting the contralateral normal prostate tissue as a control area to calculate the corresponding apparent diffusion coefficient (ADC). The ADC values were obtained by averaging three measurements to reduce measurement error. ② DCE-MRI Image Processing: On dynamic contrast-enhanced MRI images, the ROI was delineated in the lesion area, and

the time-intensity curve (TIC) type was calculated. Based on the signal enhancement pattern, TICs were classified as follows: Type I curve (slowly rising type): Signal enhancement rises slowly. Type II curve (plateau type): Signal enhancement rises and then stabilizes. Type III curve (rapid rise and fall type): Signal enhancement rises rapidly and then declines quickly. Additionally, Tissue 4D software was used to process DCE-MRI data and calculate key hemodynamic parameters, including: Ktrans: Reflects the permeability of contrast agent from capillaries into the extracellular space. Ve: Indicates the proportion of extracellular fluid, reflecting vascular permeability and the micro-environment characteristics of the lesion. Kep: Measures the rate at which contrast agent returns from the extracellular space to the intravascular compartment. For each lesion area, three ROIs were measured, and the average value was taken as the final quantitative analysis result to minimize individual differences affecting the data. To ensure objectivity and reproducibility, all images were independently reviewed in a double-blind manner by two board-certified radiologists (attending level or above), blinded to pathological outcomes. In case of disagreement, a senior radiologist mediated to reach consensus. Inter-observer agreement for ADC, Ktrans, Kep, and Ve was assessed using a two-way random-effects model with absolute agreement. According to the Landis and Koch criteria,[20] the ICC values for ADC (0.91, 95% CI: 0.87–0.94), Ktrans (0.85, 95% CI: 0.79–0.89), Kep (0.82, 95% CI: 0.76–0.87), and Ve (0.88, 95% CI: 0.83–0.92) indicated excellent agreement for ADC and good agreement for the remaining parameters.

Observation Indicators

(1) Analysis of T2WI, DWI, and DCE-MRI findings in PCA and BPL patients. (2) Comparison of DWI signal intensity values and ADC at b = 50s/mm² and b = 800s/mm² between the two groups. (3) Comparison of Ktrans, Ve, and Kep parameters in the ROIs of both groups. (4) Spearman correlation analysis of b = 50s/mm² signal intensity, b = 800s/mm² signal intensity, ADC, Ktrans, Ve, and Kep with the occurrence of PCA. (5) Receiver operating characteristic (ROC) curve analysis to evaluate the diagnostic performance and value of T2WI, DWI, and DCE-MRI alone and in combination for PCA.

Statistical Analysis

All statistical analyses were performed using GraphPad Prism 8.0 (GraphPad Software, San Diego, CA, USA) and SPSS version 25.0 (IBM Corp., Armonk, NY, USA). The distribution of continuous variables was assessed using the Shapiro–Wilk test, with all variables conforming to a normal distribution ($P > 0.05$). Outliers exceeding three standard deviations were retained as biological variation in accordance with prior literature.[21] Categorical variables were expressed as counts and percentages (n[%]) and compared using the χ^2-test. Continuous variables were presented as mean ± standard deviation (SD) and analyzed using independent samples t-tests. Correlations between imaging parameters and PCA diagnosis were evaluated using Spearman's rank correlation test. Diagnostic performance was assessed using receiver operating characteristic (ROC) curves, with the area under the curve (AUC), sensitivity, and specificity calculated for each imaging modality. For combined evaluation, the PI-RADS v2.1 scoring system was applied, using T2WI and DWI for lesions in the peripheral zone and T2WI and DCE-MRI for lesions in the transition zone, following established guidelines.[22] A two-sided P value < 0.05 was considered statistically significant.

Results

Comparison of Baseline Data

There was no significant difference between the two groups in terms of age, body mass index (BMI), prostate volume, or comorbidities ($P > 0.05$), indicating comparability. See Table 1.

Table 1 Comparison of Baseline Data ($\bar{x} \pm s$, n [%])

	PCA Group (n=33)	BPL Group (n=31)	t/x^2	*P*
Age (years)	67.28±7.84	65.93±6.59	0.743	0.460
BMI (kg/m²)	24.82±2.43	24.71±2.25	0.187	0.851
Prostate Volume (mL)	42.83±10.57	45.34±11.26	0.919	0.361

(*Continued*)

Table 1 (Continued).

	PCA Group (n=33)	BPL Group (n=31)	t/x^2	*P*
Pathological Classification	–	–	–	–
Acinar Adenocarcinoma	14 (42.42)	–	–	–
Urothelial Carcinoma	11 (33.33)	–	–	–
Ductal Adenocarcinoma	4 (12.12)	–	–	–
Adenosquamous Carcinoma	4 (12.12)	–	–	–
Comorbidities	–	–	–	–
Diabetes Mellitus	8 (24.24)	7 (22.58)	0.024	0.875
Hypertension	11 (33.33)	9 (29.03)	0.137	0.710

Analysis of T2WI, DWI, and DCE-MRI Imaging Findings

Among the 33 PCA patients, on T2WI, 16 cases of peripheral zone PCA showed patchy or nodular hypointensity, and among 11 cases of transition zone PCA, 3 exhibited large patchy hypointensity, 3 showed lenticular hypointensity with unclear boundaries, and 8 presented as small patchy or mixed signals. Five cases exhibited both peripheral and transition zone PCA with large or multiple patchy hypointensity. On DWI, 29 cases presented as patchy or nodular hyperintensity, and 4 cases showed slightly hyperintense patches, while the ADC map showed hypointensity. On DCE-MRI, PCA was characterized by early rapid and significant enhancement, followed by either sustained or decreasing enhancement. The TIC curve was classified as Type II in 21 cases and Type III in 12 cases. Among the 31 BPL patients, the transition zone on T2WI exhibited nodular mixed high and low signals, with patchy hypointensity being rare. On DWI, most cases showed iso- or slightly hyperintense signals, with 6 cases presenting as distinctly hyperintense nodules. On DCE-MRI, early-stage enhancement was markedly heterogeneous, with 17 cases exhibiting Type I TIC and 14 cases showing Type II TIC.

Comparison of DWI Signal Intensity and ADC Values at Different b-Values

The PCA group exhibited lower signal intensity values at b=50s/mm² and b=800s/mm², as well as lower ADC values compared to the BPL group ($P < 0.05$). See Table 2.

Comparison of DCE-MRI Parameters

The PCA group exhibited higher Ktrans, Ve, and Kep values on DCE-MRI compared to the BPL group ($P < 0.001$). See Table 3.

Table 2 Comparison of DWI Signal Intensity and ADC Values at Different b-Values ($\bar{x} \pm s$)

	PCA Group (n=33)	BPL Group (n=31)	*t*	*P*
b=50 s/mm²	91.28±1.65	135.36±1.87	100.139	<0.001
b=800 s/mm²	103.45±1.72	115.27±1.54	28.896	<0.001
ADC (10^{-5} mm²/s)	101.22±1.69	154.36±1.83	120.773	<0.001

Table 3 Comparison of DCE-MRI Parameters ($\bar{x} \pm s$)

	PCA Group (n=33)	BPL Group (n=31)	*t*	*P*
Ktrans (min)	0.35±0.04	0.25±0.07	7.071	0.001
Ve (min)	0.25±0.07	0.19±0.04	4.173	0.001
Kep	0.74±0.06	0.63±0.05	7.940	0.001

Correlation Analysis Between Parameters and PCA Occurrence

Spearman correlation analysis showed that signal intensity at b=50s/mm², signal intensity at b=800s/mm², and ADC levels were negatively correlated with PCA occurrence ($P < 0.05$), whereas Ktrans, Ve, and Kep levels were positively correlated with PCA occurrence ($P < 0.05$). See Table 4 and Figure 1.

lagnostic Performance and Value of T2WI, DWI, and DCE-MRI Alone and in Combination for PCA

ROC curve analysis showed that the AUCs for T2WI, DWI, and DCE-MRI in diagnosing PCA were 0.834, 0.819, and 0.696, respectively, while the combined diagnosis had an AUC of 0.902. The combination of T2WI and DWI showed higher AUC, sensitivity, specificity, and accuracy than any single modality. See Table 5 and Figure 2.

Discussion

Analysis of PCA Imaging Characteristics

PCA exhibits characteristic features in multiparametric MRI, particularly in T2WI, DWI, and DCE-MRI. In this study, PCA typically presented as patchy or nodular hypointensity on T2WI, whereas BPL predominantly showed iso- or slightly hypointense signals, in agreement with prior reports.[13,23] T2WI contrast is related to tissue water content: PCA lesions replace glandular structures with densely packed tumor cells, reducing water content and leading to low signal intensity.[24] Conversely, BPL often preserves normal gland architecture with higher water content. It should be noted, however, that prostatitis, BPH nodules, or fibrosis can also appear hypointense, which may decrease T2WI specificity.[25] Thus, relying solely on T2WI carries a risk of false-positive diagnoses, underscoring the need for combined imaging parameters.

The diagnostic role of DWI and its derived ADC has been well established.[26,27] Our data showed that both DWI signal intensity (at b = 50 and 800 s/mm²) and ADC values were significantly lower in PCA than in BPL. This reflects restricted diffusion due to high cellular density in PCA, which impedes water movement and decreases ADC values.[28] Spearman correlation analysis confirmed significant associations between PCA occurrence and both DWI intensity and ADC values ($P < 0.05$). Nonetheless, DWI has limitations—for instance, highly differentiated tumors or lesions with hemorrhage/inflammation/fibrosis may yield higher ADC values, reducing sensitivity for low-grade PCA.[29,30] Thus, combining DWI with other modalities is essential to offset these limitations.

As a key modality for assessing PCA microvascular hemodynamics, DCE-MRI revealed significantly elevated Ktrans, Ve, and Kep in PCA compared to BPL, with positive correlations to PCA occurrence ($P < 0.05$) in line with previous studies.[31] PCA typically exhibits increased angiogenesis and vascular permeability, resulting in Type II or III enhancement curves, along with elevated perfusion metrics.[32] In contrast, BPL generally shows Type I (slow-rising) enhancement curves. However, DCE-MRI is sensitive to scanning parameters, vascular status, and lesion heterogeneity —conditions such as prostatitis or hyperplasia can also elevate Ktrans or Kep, potentially reducing specificity.[33] Therefore, a combined interpretation of T2WI, DWI, and DCE-MRI is recommended to enhance diagnostic performance.

Table 4 Correlation Analysis Between Parameters and PCA Occurrence

Index	PCA Occurrence	
	r	P
b=50 s/mm²	−0.547	<0.05
b=800 s/mm²	−0.529	<0.05
ADC	−0.601	<0.05
Ktrans	0.516	<0.05
VE	0.538	<0.05
Kep	0.552	<0.05

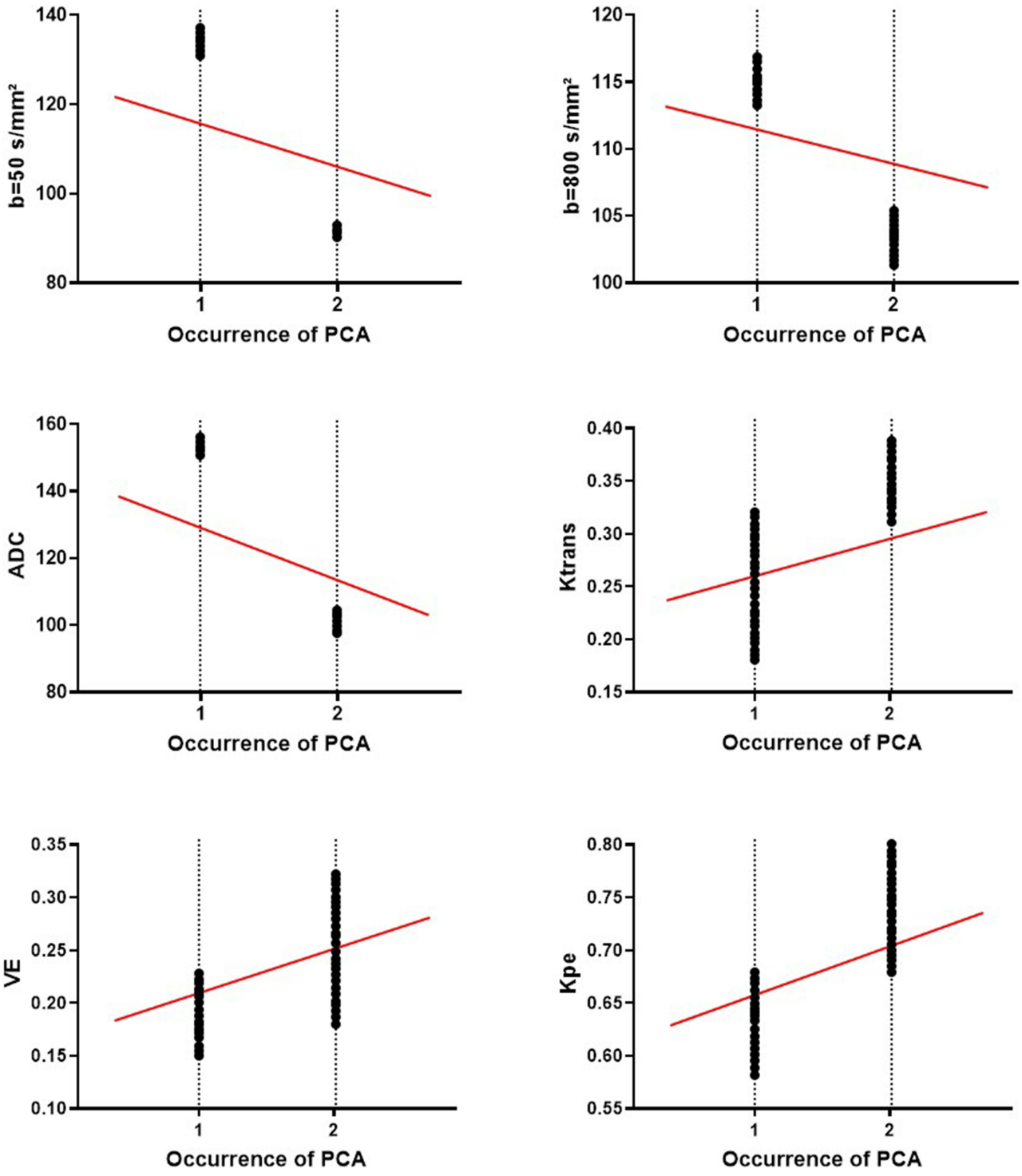

Figure 1 Scatter Plot of Correlation Analysis Between Parameters and PCA Occurrence.

Analysis of Multi-Parametric MRI Diagnostic Performance

ROC analysis demonstrated that the combined imaging model (T2WI + DWI + DCE-MRI) achieved the highest diagnostic performance with an AUC of 0.902, surpassing individual modality values (T2WI: 0.834; DWI: 0.819; DCE-MRI: 0.696). This indicates that integrating anatomical, diffusion, and perfusion imaging provides a more comprehensive lesion assessment, improving PCA detection sensitivity, specificity, and accuracy. Our findings align with broader

Table 5 Diagnostic Performance and Value of T2WI, DWI, and DCE-MRI Alone and in Combination for PCA

Index	AUC	95% CI	P	Sensitivity (%)	Specificity (%)	Accuracy (%)
T2WI	0.834	0.786–0.875	<0.05	72.67	78.59	77.32
DWI	0.819	0.772–0.853	<0.05	80.65	71.67	75.46
DCE-MRI	0.696	0.654–0.743	<0.05	76.39	63.54	66.93
Combination	0.902	0.847–0.939	<0.05	90.27	84.15	83.61

evidence that mpMRI-guided diagnostic workflows reduce unnecessary biopsies and better detect clinically significant cancer compared to PSA/DRE and biopsy-only pathways.[17,34]

Importantly, while our conclusion supports mpMRI as a valuable screening adjunct, real-world application must consider cost, accessibility, and false-positive risks. Prior studies report false-positive rates of mpMRI as high as 50%, particularly in PI-RADS 3 lesions,[35,36] leading to unnecessary biopsies. Access remains variable, especially in resource-limited settings, and high cost and requisite expertise remain barriers.[37] Additionally, advances in PSA testing, including free-to-total PSA ratio and PSAD, improve specificity and reduce overdiagnosis compared to traditional PSA or DRE alone.[38,39] Thus, mpMRI should be considered within a multimodal screening strategy, using PSA, PSAD, and mpMRI in high-risk populations to balance diagnostic accuracy and healthcare resource utilization.

Study Limitations and Future Perspectives

This study is limited by its single-center retrospective design and modest sample size, which may impede generalizability. Future research should involve prospective, multi-center studies with larger cohorts. Additionally, we did not apply PI-RADS scoring in our analysis, which is widely used for standardizing mpMRI interpretation. Future investigations should integrate PI-RADS v2.1 to enhance reproducibility.[17] Moreover, advanced analytic approaches such as radiomics or artificial intelligence integration—demonstrated in recent AI-micro-ultrasound and machine learning research—may further improve diagnostic precision and cost-effectiveness.[4,20]

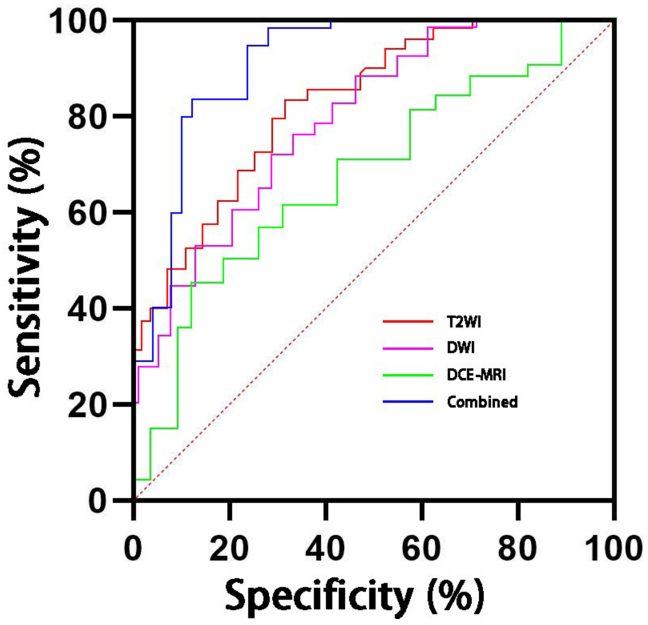

Figure 2 ROC Curves for T2WI, DWI, and DCE-MRI Alone and in Combination for PCA Diagnosis.

Conclusion

This study demonstrates that PCA exhibits characteristic features on T2WI, DWI, and DCE-MRI. The DWI signal intensity at b = 50s/mm² and b = 800s/mm², ADC values, and DCE-MRI parameters (Ktrans, Ve, Kep) are significantly correlated with PCA occurrence. The combined diagnosis using T2WI, DWI, and DCE-MRI significantly improves PCA detection rates and accuracy, providing a more reliable imaging evaluation tool for clinical practice.

However, despite the high diagnostic value of mpMRI, its clinical application should also consider real-world limitations such as high costs, limited accessibility in primary or rural settings, and the potential for false-positive findings—especially in equivocal PI-RADS 3 lesions.[3,5] These factors may affect its role as a routine screening tool for PCA.

Therefore, mpMRI is best utilized as part of a multimodal diagnostic strategy, particularly in high-risk populations or patients with elevated PSA and abnormal digital rectal exams. When integrated with PSA derivatives such as PSA density and free-to-total PSA ratio, mpMRI can enhance diagnostic accuracy while minimizing unnecessary biopsies.[28]

Future research should focus on large-scale, multicenter studies and incorporate PI-RADS scoring systems, radiomics, and artificial intelligence–based image analysis to further optimize the diagnostic pathway for PCA.

Disclosure

The author reports no conflicts of interest in this work.

References

1. Zhang K, Teoh J, Laguna P, et al. The diagnostic value of MRI for persistent prostate cancer following irreversible electroporation focal therapy. *BJU Int*. 2025;136(1):120–127. doi:10.1111/bju.16720
2. Wilson TK, Zishiri OT. Prostate Cancer: a Review of Genetics, Current Biomarkers and Personalised Treatments. *Cancer Rep*. 2024;7(10):e70016. doi:10.1002/cnr2.70016
3. Williams IS, McVey A, Perera S, et al. Modern paradigms for prostate cancer detection and management. *The Medical Journal of Australia*. 2022;217(8):424–433. doi:10.5694/mja2.51722
4. Wasim S, Lee SY, Kim J. Complexities of Prostate Cancer. *Int J Mol Sci*. 2022;23(22):14257. doi:10.3390/ijms232214257
5. Saeidi H, Ismail P, Samudi Raju C, Khairul-Asri MG, Bakrin IH. Genetic alterations in prostate cancer as diagnostic and prognostic markers. *Malaysian J Pathol*. 2023;45(2):149–155.
6. Příman O, Veselý Š, Babjuk M. New trends in prostate cancer diagnostics. *Rozhledy v chirurgii: mesicnik Ceskoslovenske chirurgicke spolecnosti*. 2022;101(3):101–107. doi:10.33699/PIS.2022.101.3.101-107
7. Presti Jr J, Alexeeff S, Avins AL. Screening for Prostate Cancer. *New Engl J Med*. 2023;389(1):93–94.
8. Padhani AR, Schoots IG. Imaging-based Diagnostic and Therapeutic Strategies for Prostate Cancer in the Coming Decades. *Radiology*. 2023;307(5):e222990. doi:10.1148/radiol.222990
9. Li X, Bai Y, Feng K, et al. Therapeutic, diagnostic and prognostic values of TRIM proteins in prostate cancer. *Pharmacological Reports: PR*. 2023;75(6):1445–1453. doi:10.1007/s43440-023-00534-9
10. Kumar Am S, Rajan P, Alkhamees M, Holley M, Lakshmanan VK. Prostate cancer theragnostics biomarkers: an update. *Investigative Clinical Urol*. 2024;65(6):527–539. doi:10.4111/icu.20240229
11. Krilaviciute A, Becker N, Lakes J, et al. Digital Rectal Examination Is Not a Useful Screening Test for Prostate Cancer. *Eur Urol Oncol*. 2023;6(6):566–573. doi:10.1016/j.euo.2023.09.008
12. Jones K, Chandran A, Rance J. Rapid diagnostic pathways for prostate cancer: a realist synthesis. *J Cancer Policy*. 2024;42:100514. doi:10.1016/j.jcpo.2024.100514
13. Inoue T, Shin T. Current magnetic resonance imaging-based diagnostic strategies for prostate cancer. *International Journal of Urology: Official Journal of the Japanese Urological Association*. 2023;30(12):1078–1086. doi:10.1111/iju.15281
14. O'Shea A, Harisinghani M. PI-RADS: multiparametric MRI in prostate cancer. *Magma (New York. Ny)*. 2022;35(4):523–532.
15. O'Connor LP, Lebastchi AH, Horuz R, et al. Role of multiparametric prostate MRI in the management of prostate cancer. *World Journal of Urology*. 2021;39(3):651–659. doi:10.1007/s00345-020-03310-z
16. Lee CH, Tan TW, Tan CH. Multiparametric MRI in Active Surveillance of Prostate Cancer: an Overview and a Practical Approach. *Korean J Radiol*. 2021;22(7):1087–1099. doi:10.3348/kjr.2020.1224
17. Lai AL, Velaga J, Tay KJ, et al. Multiparametric MRI before and after Focal Therapy for Prostate Cancer: pearls and Pitfalls for the Reporting Radiologist. *Radiol Imag Cancer*. 2025;7(2):e240269. doi:10.1148/rycan.240269
18. Keshav N, Ehrhart MD, Eberhardt SC, Terrazas MF. Local Staging of Prostate Cancer with Multiparametric MRI. *Seminars in Roentgenology*. 2021;56(4):366–375. doi:10.1053/j.ro.2021.09.001
19. Heard JR, Naser-Tavakolian A, Nazmifar M, Ahdoot M. Focal prostate cancer therapy in the era of multiparametric MRI: a review of options and outcomes. *Prostate Cancer Prostatic Dis*. 2023;26(2):218–227. doi:10.1038/s41391-022-00501-0
20. Handke AE, Ritter M, Albers P, Noldus J, Radtke JP, Krausewitz P. Prostate cancer-multiparametric MRI and alternative approaches in intervention and therapy planning. *Urologie*. 2023;62(11):1160–1168. doi:10.1007/s00120-023-02190-6
21. Goh V. PI-RADS and Multiparametric MRI: the Shape of Things to Come for Prostate Cancer. *Radiology*. 2023;307(4):e230643. doi:10.1148/radiol.230643
22. Dwivedi DK, Jagannathan NR. Emerging MR methods for improved diagnosis of prostate cancer by multiparametric MRI. *Magma*. 2022;35(4):587–608.

23. Inamura K: screening for Prostate Cancer. *New Engl J Med*. 2023;389(1):93.
24. Houshmand S, Lawhn-Heath C, Behr S. PSMA PET imaging in the diagnosis and management of prostate cancer. *Abdominal radiology (New York)*. 2023;48(12):3610–3623. doi:10.1007/s00261-023-04002-z
25. Hoover J, Butterfass C, Ponder A. Screening for Prostate Cancer. *New Engl J Med*. 2023;389(1):92–93.
26. Galosi AB, Palagonia E, Scarcella S, et al. Detection limits of significant prostate cancer using multiparametric MR and digital rectal examination in men with low serum PSA: up-date of the Italian Society of Integrated Diagnostic in Urology. *Arch Iitaliano Urol Androl*. 2021;93(1):92–100. doi:10.4081/aiua.2021.1.92
27. Fütterer JJ, Kim CK, Margolis DJ. Innovations in prostate cancer: introductory editorial. *Br J Radiol*. 2022;95(1131):20229003. doi:10.1259/bjr.20229003
28. French WW, Wallen EM. Advances in the diagnostic options for prostate cancer. *Postgraduate Medicine*. 2020;132(sup4):52–62. doi:10.1080/00325481.2020.1822067
29. Chung Y, Hong SK. Evaluating prostate cancer diagnostic methods: the role and relevance of digital rectal examination in modern era. *Investigative Clinical Urol*. 2025;66(3):181–187. doi:10.4111/icu.20240456
30. Chandra Engel J, Eklund M, Jäderling F, et al. Diagnostic Effects of Omitting Systematic Biopsies in Prostate Cancer Screening. *Eur Urol Oncol*. 2025;8(2):435–443. doi:10.1016/j.euo.2024.10.002
31. Bass EJ, Pantovic A, Connor M, et al. A systematic review and meta-analysis of the diagnostic accuracy of biparametric prostate MRI for prostate cancer in men at risk. *Prostate Cancer Prostatic Dis*. 2021;24(3):596–611. doi:10.1038/s41391-020-00298-w
32. Costa DN. Multiparametric MRI of the Prostate: beyond Cancer Detection and Staging. *Radiology*. 2021;299(3):624–625. doi:10.1148/radiol.2021204506
33. Bryce C, Rapp A. Multiparametric MRI for the Evaluation of Prostate Cancer. *Am Family Phys*. 2022;105(6):665–666.
34. Brondani Torri G, Antune Pereira P, Piovesan Wiethan C, et al. Comparison of Multiparametric MRI and the Combination of PSMA Plus MRI for the Intraprostatic Diagnosis of Prostate Cancer: a Systematic Review and Meta-Analysis. *Clinical Nuclear Medicine*. 2024;49(8):e375–e382. doi:10.1097/RLU.0000000000005265
35. Aguirre DA, Cardona Ortegón JD. Unlocking the Benefits of Multiparametric MRI for Predicting Prostate Cancer Recurrence. *Radiology*. 2023;309(2):e232819. doi:10.1148/radiol.232819
36. Şahin Y, Şahin A, Çelik M A case report: application of 68Ga-PSMA-PET/CT for the diagnosis of bone metastases in patients with low prostate-specific antigen levels. *J Mod Med Oncol*. 2022;2:2. doi:10.53964/jmmo.2022002
37. Barone B, Napolitano L, Calace FP, et al. Reliability of Multiparametric Magnetic Resonance Imaging in Patients with a Previous Negative Biopsy: comparison with Biopsy-Naïve Patients in the Detection of Clinically Significant Prostate Cancer. *Diagnostics*. 2023;13(11):1.
38. Massanova M, Vere R, Robertson S, et al. Clinical and prostate multiparametric magnetic resonance imaging findings as predictors of general and clinically significant prostate cancer risk: a retrospective single-center study. *Curr Urol*. 2023;17(3):147–152. doi:10.1097/CU9.0000000000000173
39. Crocetto F, Barone B, De Luca L, Creta M. Granulomatous prostatitis: a challenging differential diagnosis to take into consideration. *Future Oncology*. 2020;16(13):805–806. doi:10.2217/fon-2020-0185